

Soft Matter

Accepted Manuscript



This is an *Accepted Manuscript*, which has been through the Royal Society of Chemistry peer review process and has been accepted for publication.

Accepted Manuscripts are published online shortly after acceptance, before technical editing, formatting and proof reading. Using this free service, authors can make their results available to the community, in citable form, before we publish the edited article. We will replace this *Accepted Manuscript* with the edited and formatted *Advance Article* as soon as it is available.

You can find more information about *Accepted Manuscripts* in the [Information for Authors](#).

Please note that technical editing may introduce minor changes to the text and/or graphics, which may alter content. The journal's standard [Terms & Conditions](#) and the [Ethical guidelines](#) still apply. In no event shall the Royal Society of Chemistry be held responsible for any errors or omissions in this *Accepted Manuscript* or any consequences arising from the use of any information it contains.

Effects of topological constraints on globular polymers

Maxim V. Imakaev,^a Konstantin M. Tchourine,^b Sergey Nechaev,^{*c,d,e} and Leonid A. Mirny^{*a,f}

Received Xth XXXXXXXXXXXX 20XX, Accepted Xth XXXXXXXXXXXX 20XX

First published on the web Xth XXXXXXXXXXXX 200X

DOI: 10.1039/b000000x

Topological constraints can affect both equilibrium and dynamic properties of polymer systems, and can play a role in the organization of chromosomes. Despite many theoretical works, the effects of topological constraints on the equilibrium state of a single compact polymer have not been systematically studied. Here we use simulations to address this longstanding problem. We find that sufficiently long unknotted polymers differ from knotted ones in the spatial and topological states of their subchains. The unknotted globule has subchains that are mostly unknotted and form asymptotically compact $R_G(s) \sim s^{1/3}$ crumples. However, crumples display high fractal dimension of the surface $d_b = 2.8$, forming excessive contacts and interpenetrating each other. We conclude that this topologically constrained equilibrium state resembles a conjectured crumpled globule [Grosberg *et al.*, *Journal de Physique*, 1988, **49**, 2095], but differs from its idealized hierarchy of self-similar, isolated and compact crumples.

1 Introduction

Topological constraints, i.e. the inability of chains to pass through each other, have significant effects on both equilibrium and dynamic properties of polymer systems^{1–3} and can play important roles in the organization of chromosomes^{3–6}. Early theoretical works suggested that topological constraints *per se* compress polymer rings or polymer subchains by topological obstacles imposed by surrounding subchains^{7–9}. This compression makes a subchain of length s form a space-filling configuration that has an average radius of gyration $R_G(s) \sim s^{1/3}$. Recent simulations of topologically constrained unconcatenated polymer rings in a melt^{10–14} have demonstrated the effect of compression into space-filling configurations and confirmed $s^{1/3}$ scaling, thus providing strong support to early conjectures.

The role of topological constraints in the *equilibrium* state of a single compact and unknotted polymer remains unknown. Earlier works^{3,7,8} have put forward a concept of the *crumpled globule* as the equilibrium state of a compact and unknotted polymer. In the crumpled globule, the subchains were suggested to be space-filling and unknotted. This conjecture remained untested for the quarter of the century. Here, we test

this conjecture by comparing equilibrium compact states of a topologically constrained and unknotted polymer, referred to below as the *unknotted globule*, with those a topologically relaxed one, referred to below as the *knotted globule* (Fig. 1).

Recent computational studies examined the role of topological constraints in the *non-equilibrium* (or quasi-equilibrium) polymer states that emerge upon polymer collapse^{15–19}. This non-equilibrium state, often referred to as the *fractal globule*^{6,15}, can indeed possess some properties of the conjectured equilibrium crumpled globule. Properties of the fractal globule, its stability²⁰, and its connection to the equilibrium state are yet to be understood.

Elucidating the role of topological constraints in equilibrium and non-equilibrium polymer systems is important for understanding organization of chromosomes. Long before experimental data on chromosome organization became available¹⁵, the crumpled globule was suggested as a state of long DNA molecules inside a cell³. Recent progress in microscopy²¹ and genomics²² provided new data on chromosome organization that appear to share several features with topologically constrained polymer systems^{15,23,24}. For example, segregation of chromosomes into territories resembles segregation of space-filling rings^{5,12}, while features of intra-chromosomal organization revealed by Hi-C technique are consistent with a non-equilibrium fractal globule emerging upon polymer collapse^{6,15,25} or upon polymer decondensation²³. These findings suggest that topological constraints can play important roles in the formation of chromosomal architecture⁴.

Here we examine the role of topological constraints in the equilibrium state of a compact polymer (Fig. 1). We perform equilibrium Monte Carlo simulations of a confined unentangled polymer ring with and without topological constraints.

^aDepartment of Physics, MIT, Cambridge, MA 02139, USA

^bCenter for Genomics and Systems Biology, New York University, New York, USA

^cUniversité Paris-Sud/CNRS, LPTMS, UMR8626, Bât. 100, 91405 Orsay, France

^dP.N.Lebedev Physical Institute of the Russian Academy of Sciences, 119991, Moscow, Russia

^eNational Research University Higher School of Economics, 109028 Moscow, Russia

^fInstitute for Medical Engineering and Science, MIT, Cambridge, MA 02139, USA

Without topological constraints a polymer forms a classical equilibrium globule with a high degree of knotting^{26,27}. A polymer is kept in the globular state by impermeable boundaries, rather than pairwise energy interactions, allowing fast equilibration at a high volume density.

We find that topological states of closed subchains (loops) are drastically different in the two types of globules and reflect the topological state of the whole polymer. Namely, loops of the unknotted globule are only weakly knotted and mostly unconcatenated. We also find that spatial characteristics of small knotted and unknotted globules are very similar, with differences starting to appear only for sufficiently large globules. Subchains of these large unknotted globules become asymptotically compact ($R_G(s) \sim s^{1/3}$), forming crumples. Analyses of the fractal dimension of surfaces of loops suggest that crumples form excessive contacts and interpenetrate each other. Overall, the asymptotic behavior we find support the conjectured crumpled globule concept⁷. However, our results also demonstrate that the internal organization of the unknotted globule at equilibrium differs from an idealized hierarchy of self-similar isolated compact crumples.

2 Results

2.1 Model

A single homopolymer ring with excluded volume interactions was modeled on a cubic lattice and confined into a cubic container at volume density 0.5. The Monte Carlo method with non-local moves²⁸ allowed us to study chains up to $N = 256\,000$. If monomers were prohibited to occupy the same site, this Monte Carlo move set naturally constrains topology, and the polymer remains unknotted. Setting a small finite probability for two monomers to occupy the same lattice site would let two regions of the chain cross. This would relax topological constraints while largely preserving the excluded volume (Fig. S7). The topological state of a loop was characterized by \varkappa , the logarithm of the Alexander polynomial evaluated at -1.1 ^{27,29,30}. To ensure equilibration, we estimated the scaling of the equilibration time with N for $N \leq 32\,000$, extrapolated it to large N , and ran simulations of longer chains, $N = 108\,000$ and $256\,000$, to exceed the estimated equilibration time (see Supplement and Fig. S9 for details). We also made sure that chains with topological constraints remain completely unknotted through the simulations, while polymers with relaxed topological constraints become highly entangled²⁷ (Fig. S8)

2.2 Topological properties

First, we asked how the topological state of the whole polymer influences the topological properties of its subchains. Be-

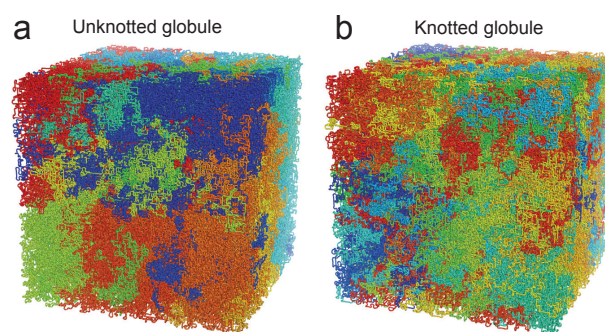


Fig. 1 Representative conformations of two different types of globules (confined polymer rings, length $N = 256\,000$): (a) the unknotted globule formed by a single polymer ring with topological constraints; (b) the knotted globule formed by a polymer ring without topological constraints. Both chains are painted in red-yellow-green-blue along the polymer length.

cause a topological state can be rigorously defined only for a closed contour, we focused our analysis on loops, i.e. subchains with two ends occupying neighboring lattice sites. Fig. 2a presents the average knot complexity $\langle \varkappa(s) \rangle$ for loops of length s for both types of globules. We found that loops of the knotted globule were highly knotted, with the knot complexity rising sharply with s . Loops of the unknotted globule, on the contrary, were weakly knotted, and their complexity increased slowly with length. Their knotting complexity was also very variable, indicating the abundance of slip knots³¹ (Fig. S5).

This striking difference in the topological states of loops for globally knotted and unknotted chains is a manifestation of the general statistical behavior of so-called matrix-valued Brownian Bridges (BB)³². The knot complexity \varkappa of loops in the topologically unconstrained globule is expected to grow as $\varkappa(s) \sim s^2$. Contrarily, due to the global topological constraint imposed in the unknotted globule, the knot complexity of its loops grows slower, $\varkappa(s) \sim s$, which follows from the statistical behavior of BB in spaces of constant negative curvature (see Appendix, Fig. 2a, and³²⁻³⁵ for details). Our simulations are in good agreement with this theory (Fig. 2a).

Another topological property of loops of a globule is a degree of concatenation between the loops. We computed the linking number for pairs of non-overlapping loops in each globule (Fig. 2b) and found that loops in the unknotted globule are much less concatenated than loops in the knotted globule.

Taken together, these results show that the topological state of the whole (“parent”) chain propagates to the “daughter” loops. While loops of the unknotted globule are linked and knotted, their degree of entanglement is much lower than that in the topologically relaxed knotted globule (Fig. S5). Our results also demonstrate that loops of a single unknotted globule are not equivalent to recently studied rings in a melt, which

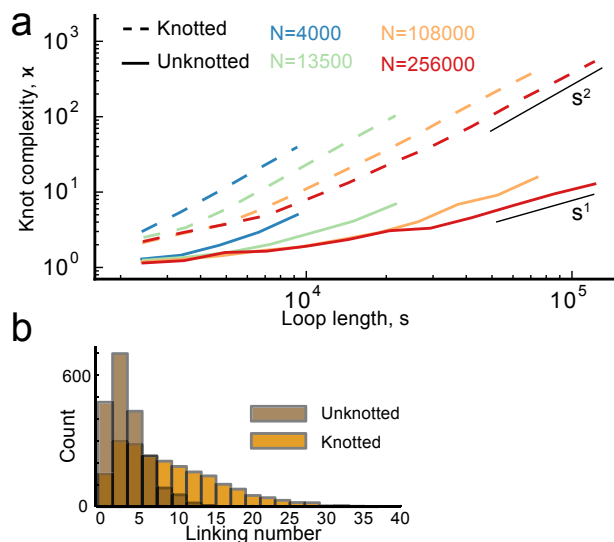


Fig. 2 Topological properties of polymer loops in the knotted and unknotted globules. (a) Knot complexity of polymer loops as a function of their length, s , for chains of different length N (shown by colors) in knotted (dashed) and unknotted (solid) globules. (b) Distribution of the linking numbers for non-overlapping loops of length $s = 9000$ to 11000 in 32000-long globules.

were unknotted and unconcatenated. We further examine this parallel below.

2.3 Spatial properties

Next, we examined the effects of topological constraints on the spatial properties of loops. We computed an average gyration radius $R_G(s)$ (Fig. 3) as a function of loop length s , in chains of different length N . The two types of globules show different trends in $R_G(s)$.

The behavior of $R_G(s)$ for knotted globules has two regimes that are well-known and described by the Flory theorem³⁶. Shorter subchains behave as Gaussian coils $R_G(s) \sim s^{1/2}$ until they reach the confining walls at $R \sim N^{1/3}$, i.e. for $s \lesssim s_c \sim N^{2/3}$. For longer subchains, $s \gtrsim s_c$, $R_G(s)$ plateaus at $R_G(s) \sim N^{1/3}$. Note that this is qualitatively similar to $R_G(s)$ for a phantom chain confined to a box (Fig. S1). Overall, for knotted globules, our results are in line with theoretical predictions.

Subchains in unknotted globules were proposed to be compressed by topological constraints and follow $R_G(s) \sim s^{1/3}$ relation⁷. Surprisingly, we do not observe any significant compression of loops in chains of length $N \leq 13500$, as there is little difference between $R_G(s)$ curves for the two types of globule. For longer chains, $N \geq 10^5$, we observe increasing difference between $R_G(s)$ of knotted and unknotted globules. Little difference is seen in other moments of the distribution

of subchain sizes (Fig. S3). In the unknotted globules, we observe a range of subchain length, $10^3 \leq s \leq 10^4$, in which the subchains are compressed ($R_G(s) \sim s^{1/3}$) and the curves for the two largest systems collapse. However, this scaling regime arises as a gradual decrease from $R_G(s) \sim s^{1/2}$ (see Fig. S11), and thus cannot be established unambiguously.

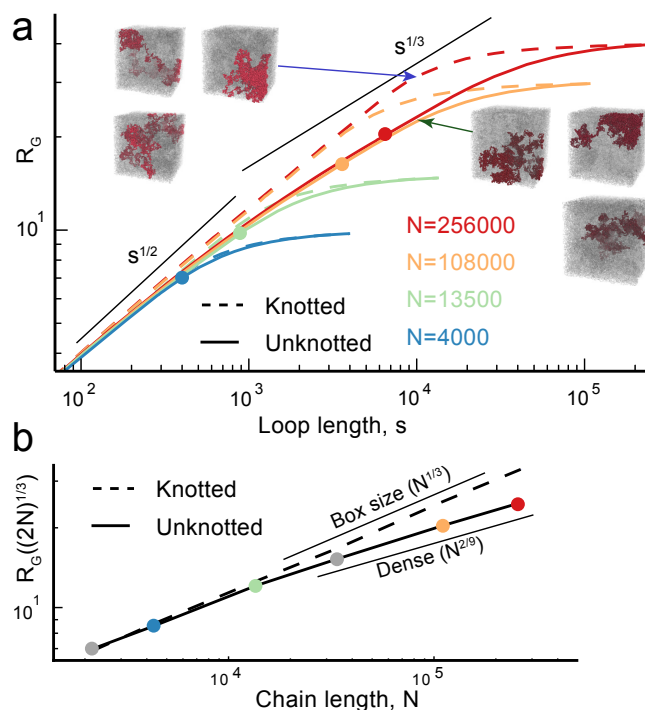


Fig. 3 Spatial properties of loops in the knotted and unknotted globules. (a) The average radius of gyration $R_G(s)$ for loops of length s . Inset shows conformations of three 10000-monomer loops for $N = 256000$ globules. Circles indicate subchains of length $(2N)^{2/3}$, which is equal to L^2 , squared box size. (b) Dependence of $R_G(s = (2N)^{2/3})$ on the chain size N . Colored circles match to circles in the Fig. 3a; grey circles denote $N = 2000$ and $N = 32000$, which are not shown in the Fig. 3a.

Earlier studies have established that topological constraints become relevant for chains that are several times longer than a characteristic length N_e called the entanglement length^{4,36–38}. For a similar system, an equilibrium melt of rings at the same volume density, it was estimated that $N_e \approx 175^{11}$, and topological constraints become relevant only above several N_e , i.e. for $N \gtrsim 1000^{11}$. Following this logic, we expect that in our system topological constraints become relevant for subchains of length $s \gtrsim 1000$. However, subchains $s \geq s_c$ experience confinement, which overshadows topological compression. Indeed, when we consider only loops not touching the boundary, we see the difference for subchains $s \gtrsim 1000$ (Fig. S4). For topological constraints to be relevant, a polymer should have subchains that do not experience external confinement

($s \leq s_c \sim N^{2/3}$) but are sufficiently long to experience topological compression ($s \gtrsim 1000$). This sets a lower limit for a polymer to experience topological constraints ($N^{2/3} \gtrsim 1000$). Consistently, we observe a difference between $R_G(s)$ for the two types of globules for $N \gtrsim 32000$ (Fig. 3a, S11).

To test the conjecture that $R_G(s) \sim s^{1/3}$, we need to separate compression by topological constraints from the effect of confinement. To this end, we focused on loops of size $s = s_c$, which are the largest loops not affected by confinement. Fig. 3b presents $R_G(s_c)$ as a function of N and clearly shows distinct scalings for knotted and unknotted globules. The knotted globule follows $R_G(s_c) \sim N^{1/3}$, which is a consequence of $R_G(s) \sim s^{1/2}$. For the unknotted globule, however, we observe $R_G(s_c) \sim N^{2/9}$, which corresponds to $R_G(s) \sim s^{1/3}$. Thus, in agreement with earlier conjectures^{7,33}, topological constraints lead to the formation of "space-filling" subchains, i.e. $R(s) \sim s^{1/3}$. However, the compressing effect of topological constraints becomes evident only for very long polymers, such as $N \gtrsim 10^5$. Space-filling crumples are visible in unknotted globules of length $N = 256000$, but the difference is visually subtle (Fig. 4). Distinguishing individual knotted and unknotted globules by eye is challenging, but a pattern is visible when several globules are compared.

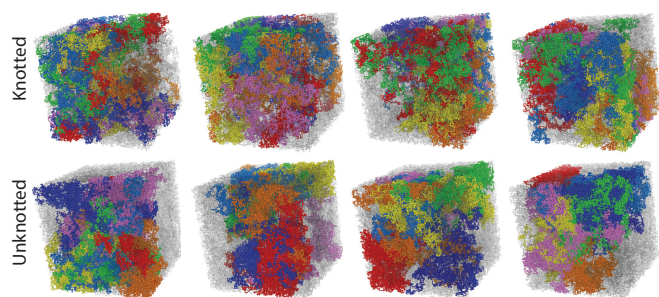


Fig. 4 Compression of subchains in unknotted loops. Seven consecutive subchains of length $s = 10000$ are highlighted with consecutive colors (red, orange, yellow, green, marine, blue, violet) in four knotted and unknotted $N = 256000$ long globules; rest of the chain is shown in grey.

Our analysis reveals significant effects of global topological constraints on the topological and spatial characteristics of loops. Next, we asked whether topological states and sizes of loops are intrinsically connected. We computed R_G and \varkappa for loops of length $s = 20000$ in $N = 256000$ globules (Fig. S6). Despite having similar R_G , loops from the two types of globules show different knot complexity: all loops from the unknotted globule were significantly less knotted than loops of the same length in the knotted globule. Moreover, \varkappa for loops in the knotted globule negatively correlates with R_G : more compact loops form more complex knots in the system where no topological constraints were present. This relationship, however, does not hold across globules: loops in the un-

knotted globule are on average more compact and less knotted. These observations highlight that there is no simple relationship between spatial and topological properties of closed contours.

2.4 Contact probability

Another important characteristic of internal polymer organization is the probability $P_c(s)$ of a contact between two monomers separated by a contour length s . For example, for a 3D random walk, $P_{c,RW}(s) \sim s^{-3/2}$ (see Supplemental Information). Recently developed experimental technique, Hi-C, measures $P_c(s)$ experimentally for chromosomes inside cells^{15,22}. Comparison of experimental and theoretical $P_c(s)$ can shed light on polymer organization of chromosomes^{15,39,40}. In our previous work, we found that a non-equilibrium fractal globule, which emerges upon a polymer collapse, has $P_c(s) \sim s^\alpha$, $\alpha \approx -1$. The $P_c(s)$ scaling for the fractal globule agrees with $P_c(s)$ from the Hi-C data for human chromosomes better than other polymer ensembles¹⁵.

Figure 5 presents $P_c(s)$ for the knotted and unknotted globules. For the knotted globule, as expected, we observed two regimes $P_c(s) \sim s^{-3/2}$ for $s \lesssim s_c$, followed by a plateau for $s \gtrsim s_c$ ⁴¹. As above, an equilibrium globule without topological constraints can be considered as a "gas of random walks"⁴¹, i.e. short chains ($s \lesssim s_c$) behave as random walks. Different random walks are mixed and are equally likely to contact each other, leading to the plateau of $P_c(s)$ for $s \gtrsim s_c$. Subchains in the unknotted globule, however, experience additional confinement by topological constraints and have a different $P_c(s)$. For $N \leq 13500$, little difference is observed between the two types of globules, which is consistent with our observation that topological effects play little role for shorter polymers.

Longer unknotted globules show a different $P_c(s)$ curve with a less steep decline of $P_c(s)$ for small s and no distinct plateau for large s . $P_c(s)$ plots and their derivatives (Fig. S11) suggest a possible scaling regime $P_c(s) \sim s^\alpha$, $-1 < \alpha < -0.8$ for loops of $s = 10^3 - 10^4$, where topological constraints are expected to play a bigger role. The value observed for the melt of rings^{11,12}, $\alpha \approx -1.17$, is outside of this range highlighting a difference between these systems.

Note, however, that estimating scaling of $P_c(s)$ for both types of globules is challenging due to a broad transition between different regimes and the effects of confinement. As seen on Fig. S11, even for the knotted globule, where the scaling of $P_c(s) \sim s^{-3/2}$ is known, it can be observed only asymptotically.

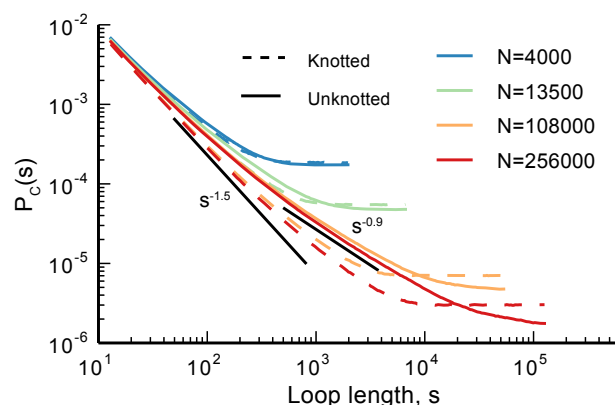


Fig. 5 Scaling of the contact probability. $P_c(s)$ is shown for knotted and unknotted globules of different sizes. Compare to Fig. 3a.

2.5 Fractal structure of loops

Loops of the unknotted globule become asymptotically compact as the polymer size increases, forming crumples. The question that follows is whether such crumples become more isolated from each other. To answer this question, we studied shapes of crumples formed by loops; we calculated the fractal dimension of their surface and corrected for finite-size effects. For a loop, the surface area of the boundary, A , is defined as the number of monomers forming contacts with the rest of the polymer⁴. The fractal dimension of the loop boundary, d_b , is defined by $A(s) \sim s^{d_b/3}$. Note that d_b denotes fractal dimension of the boundary only in the compact subchain regime, $R_G \sim s^{1/3}$; for non-compact subchains it measures the scaling of the subchain boundary with subchain length.

Finite-size effects, i.e. effects of the global confinement on the loops, can be taken into account by a function that depends on the fraction of the loop s in the whole chain N , $f(\frac{s}{N})$, giving the surface area $A(s, N) = f(\frac{s}{N}) s^{d_b/3} = g(\frac{s}{N}) N^{d_b/3}$. We can then compute d_b by comparing A for chains with the same value of s/N , but in globules of different length N (Fig. 6a). Figure 6b shows d_b as a function of N and gives asymptotic behavior of d_b for large N , where topological constraints become most relevant. As expected, loops in the knotted globule have $d_b \approx 3$, suggesting that loops fully mix with each other throughout their entire volume. In the unknotted globule, however, loops have $d_b \approx 2.8$, indicating that loops are not fully mixed, yet not fully isolated. A fractal dimension $d_b = 2$ would indicate interactions over two-dimensional surface area, i.e. as bricks stacked together. This result is also consistent with the fractal dimension of a ring surface ≈ 2.85 found for unconcatenated rings in a melt¹², and suggests that loops of the unknotted globule are not isolated, and form interdigitated compact crumples (Fig. 4).

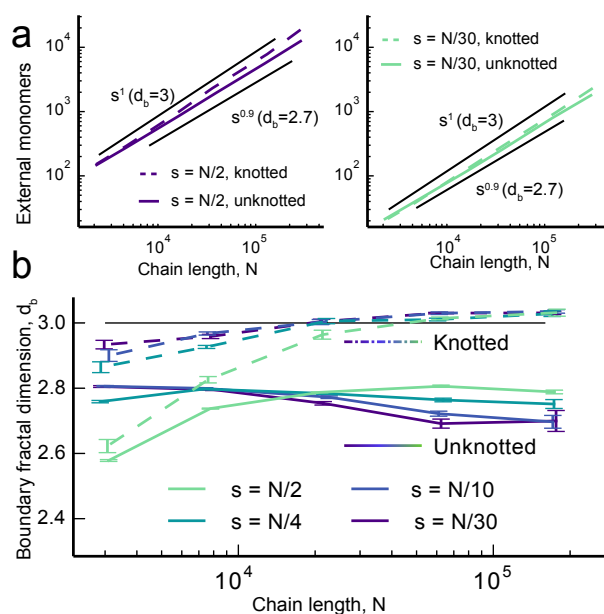


Fig. 6 Fractal dimension of a loop surface. (a) The surface area $A(s, N)$ of loops of length $N/2$ (left) and $N/30$ (right) as a function of chain length N . (b) The fractal dimension of the surface measured from slopes in (a), as a function of N . The slope in (a) is estimated from pairwise differences between two neighboring values of N . Error bars show a standard error of the mean obtained by bootstrapping. To allow comparisons between error bars, plots were shifted by a negligible offset along the horizontal axis.

3 Conclusions

Our results provide strong support to the early conjecture⁷ and reveal several new insights about the effects of topological constraints on the compact state of a polymer. In agreement with⁷, we observe that topological constraints make a compact polymer acquire a new conformational state, earlier called the crumpled globule. In this state, the unknotted polymer forms largely unknotted and weakly concatenated crumples. These crumples are asymptotically compact ($R_G(s) \sim s^{1/3}$) and differ from random walk subchains ($R_G(s) \sim s^{1/2}$) emerging in the absence of topological constraints. However, the effect is hard to detect, since large subchains experience confinement, while small subchains (less than a few N_e) do not feel topological constraints. As a result, only chains of some intermediate size ($10^3 \lesssim s \lesssim N^{2/3}$) form topologically compressed crumples. Similarly, the effects of topological constraints are most evident in large globules ($N \gtrsim 10^5$).

Unexpectedly, we also found that the loops in a globally unknotted polymer are somewhat knotted and concatenated. The brownian bridge argument explains this phenomenon and is in good quantitative agreement with the scaling of $\varkappa(s)$ (Fig. 2). Knots formed by loops of the unknotted globule are much less

complex than those in the topologically unconstrained globule. Overall, this demonstrates how global topological constraints imposed in the whole chain propagate into local topological constraints acting on its subchains.

We found little evidence of the predicted self-similarity in the internal organization of the unknotted globule. Even the largest system considered ($N = 256\,000$) shows a rather narrow (factor of 10 in s) scaling regime in $R_G(s)$. Moreover, the fractal dimension of loop surfaces, $d_b \approx 2.8$, shows that compact crumples are neither fully isolated ($d_b = 2$), nor fully mixed ($d_b = 3$). Some degree of mixing with neighboring subchains makes crumples swell, possibly narrowing the range of s where subchains are self-similar, and further highlighting differences between a finite-size unknotted globule and an idealized hierarchical crumpled globule proposed theoretically⁷.

It is possible that features of the conjectured crumpled globule can be more evident in a non-equilibrium state that emerges immediately after polymer collapse (often referred to as the fractal globule)^{6,15}, rather than in the equilibrium system considered here. In the non-equilibrium state, a broader regime of scaling in $P_c(s)$ and $R_G(s)$ suggests that even much shorter chains have self-similar organization (see also⁴). We cannot rule out the possibility that effects other than topological constraints, acting on shorter time scales, constraint a collapsed chain in a quasi-equilibrium or transient state. If it exists, such a state would be different from the crumpled globule studied here.

We find many similarities and some notable differences between the unknotted globule formed by a single ring and the melt of unconcatenated rings^{11,12}. Both systems show quantitatively similar compression of rings and loops by topological interactions, as follows from similar $R_G(s)$ asymptotic scalings and similar fractal dimension of the surface. The systems however are different on many levels. While rings in a melt are monodispersed, unknotted and unconcatenated, loops of a single polymer have a broad size distribution, are knotted and concatenated. This variation in size can lead to swelling of larger loops. Moreover, larger loops experience global confinement of the globule. Topologically, the systems are different since considered polymer ring has only one global topological constraint, while the melt has as many constraints as the number of rings. Nevertheless some characteristics of mid-size loops in unknotted globules resemble those of rings in a melt.

Overall, we find that equilibrium state of a single unknotted polymer chain is different from topologically relaxed system. It would be interesting to see whether and to what extent this phenomenon is observed in other physical systems where topology can play a role.

4 Acknowledgments

This work was supported by MIT-France Seed Funds and NCI-funded Center for Physical Sciences in Oncology at MIT (U54CA143874). We are grateful to Geoffrey Fudenberg, Anton Goloborodko and Christopher McFarland for many productive discussions and to Alexander Y. Grosberg for his feedback and suggestions. S.N. acknowledges the support of the Higher School of Economics program for Basic Research.

References

- 1 A. D. Bates and A. Maxwell, *DNA topology*, Oxford university press, 2005.
- 2 K. V. Klenin, A. V. Vologodskii, V. V. Anshelevich, A. M. Dykhne and M. D. Frank-Kamenetskii, *Journal of Biomolecular Structure and Dynamics*, 1988, **5**, 1173–1185.
- 3 A. Grosberg, Y. Rabin, S. Havlin and A. Neer, *EPL (Europhysics Letters)*, 1993, **23**, 373.
- 4 J. D. Halverson, J. Smrek, K. Kremer and A. Y. Grosberg, *Reports on Progress in Physics*, 2014, **77**, 022601.
- 5 J. Dorier and A. Stasiak, *Nucleic acids research*, 2009, **37**, 6316–6322.
- 6 L. A. Mirny, *Chromosome research*, 2011, **19**, 37–51.
- 7 A. Y. Grosberg, S. K. Nechaev and E. I. Shakhnovich, *Journal de physique*, 1988, **49**, 2095–2100.
- 8 A. Khokhlov and S. Nechaev, *Physics Letters A*, 1985, **112**, 156–160.
- 9 M. Cates and J. Deutsch, *Journal de physique*, 1986, **47**, 2121–2128.
- 10 D. Reith, L. Mirny and P. Virnau, *Progress of Theoretical Physics Supplement*, 2011, **191**, 135–145.
- 11 T. Vettorel, A. Y. Grosberg and K. Kremer, *Physical biology*, 2009, **6**, 025013.
- 12 J. D. Halverson, W. B. Lee, G. S. Grest, A. Y. Grosberg and K. Kremer, *The Journal of chemical physics*, 2011, **134**, 204904.
- 13 J. Suzuki, A. Takano, T. Deguchi and Y. Matsushita, *The Journal of chemical physics*, 2009, **131**, 144902.
- 14 A. Rosa and R. Everaers, *arXiv preprint arXiv:1310.7641*, 2013.
- 15 E. Lieberman-Aiden, N. L. van Berkum, L. Williams, M. Imakaev, T. Ragoczy, A. Telling, I. Amit, B. R. Lajoie, P. J. Sabo, M. O. Dorschner *et al.*, *science*, 2009, **326**, 289–293.
- 16 V. G. Rostiashvili, N.-K. Lee and T. A. Vilgis, *The Journal of chemical physics*, 2002, **118**, 937–951.
- 17 C. F. Abrams, N.-K. Lee and S. Obukhov, *EPL (Europhysics Letters)*, 2002, **59**, 391.

- 18 B. Chu, Q. Ying and A. Y. Grosberg, *Macromolecules*, 1995, **28**, 180–189.
- 19 A. Chertovich and P. Kos, *The Journal of chemical physics*, 2014, **141**, 134903.
- 20 R. D. Schram, G. T. Barkema and H. Schiessel, *The Journal of chemical physics*, 2013, **138**, 224901.
- 21 Y. Markaki, M. Gunkel, L. Schermelleh, S. Beichmanis, J. Neumann, M. Heidemann, H. Leonhardt, D. Eick, C. Cremer and T. Cremer, Cold Spring Harbor symposia on quantitative biology, 2011, pp. sqb–2010.
- 22 J. Dekker, M. A. Marti-Renom and L. A. Mirny, *Nature Reviews Genetics*, 2013.
- 23 A. Rosa and R. Everaers, *PLoS computational biology*, 2008, **4**, e1000153.
- 24 A. Y. Grosberg, *Polymer Science Series C*, 2012, **54**, 1–10.
- 25 V. A. Avetisov, V. Ivanov, D. Meshkov and S. Nechaev, *JETP letters*, 2013, **98**, 242–246.
- 26 I. Lifshitz, A. Y. Grosberg and A. Khokhlov, *Reviews of Modern Physics*, 1978, **50**, 683.
- 27 P. Virnau, Y. Kantor and M. Kardar, *Journal of the American Chemical Society*, 2005, **127**, 15102–15106.
- 28 T. Vettorel, S. Y. Reigh, D. Y. Yoon and K. Kremer, *Macromolecular rapid communications*, 2009, **30**, 345–351.
- 29 R. C. Lua and A. Y. Grosberg, *PLoS computational biology*, 2006, **2**, e45.
- 30 P. Virnau, L. A. Mirny and M. Kardar, *PLoS computational biology*, 2006, **2**, e122.
- 31 J. I. Sułkowska, E. J. Rawdon, K. C. Millett, J. N. Onuchic and A. Stasiak, *Proceedings of the National Academy of Sciences*, 2012, **109**, E1715–E1723.
- 32 S. Nechaev, A. Y. Grosberg and A. Vershik, *Journal of Physics A: Mathematical and General*, 1996, **29**, 2411.
- 33 S. Nechaev and O. Vasilyev, *Journal of Knot Theory and Its Ramifications*, 2005, **14**, 243–263.
- 34 S. Nechaev and Y. G. Sinai, *Boletim da Sociedade Brasileira de Matemática-Bulletin/Brazilian Mathematical Society*, 1991, **21**, 121–132.
- 35 H. Furstenberg, *Transactions of the American Mathematical Society*, 1963, 377–428.
- 36 P.-G. De Gennes, *Scaling concepts in polymer physics*, Cornell university press, 1979.
- 37 A. Y. Grosberg and A. R. Khokhlov, *Statistical physics of macromolecules*, American Institute of Physics New York, 1994.
- 38 R. Everaers, S. K. Sukumaran, G. S. Grest, C. Svaneborg, A. Sivasubramanian and K. Kremer, *Science*, 2004, **303**, 823–826.
- 39 N. Naumova, M. Imakaev, G. Fudenberg, Y. Zhan, B. R. Lajoie, L. A. Mirny and J. Dekker, *Science*, 2013, **342**, 948–953.
- 40 T. B. Le, M. V. Imakaev, L. A. Mirny and M. T. Laub, *Science*, 2013, **342**, 731–734.
- 41 R. Lua, A. L. Borovinskiy and A. Y. Grosberg, *Polymer*, 2004, **45**, 717–731.
- 42 G. Kolesov, P. Virnau, M. Kardar and L. A. Mirny, *Nucleic acids research*, 2007, **35**, W425–W428.

Appendix

Statistics of matrix-valued Brownian Bridges

The conditional distributions of a knot complexity of a subpart of a globally unknotted polymer chain is typical problem in the theory of Markov chains and deals with the determination of the conditional probability for so-called *Brownian Bridges* (BB). The investigation of statistics of BB supposes the determination of the probability $P(\mathbf{x}, t | \mathbf{0}, T)$ for a random walk to start at the point $\mathbf{x} = \mathbf{0}$, to visit the point \mathbf{x} at some intermediate moment $0 < t < T$, and to return to the initial point $\mathbf{x} = \mathbf{0}$ at the moment T . The same question can be addressed for BB on the graphs of noncommutative groups, on Riemann surfaces and for products of random matrices of groups^{32,34}.

Our topological problem to determine the complexity of a subloop in a globally trivial collapsed polymer chain, allows natural interpretation in terms of BB. Suppose the following imaginative experiment. Consider the phase space Ω of all topological states of densely packed knots on the lattice. Select from Ω the subset ω of trivial knots. To simplify the setting, consider a knot represented by a braid, as shown in the Fig. 7, where the braid is depicted by a sequence of uncorrelated "black boxes" (each black box contains some number of over- and under-crossings). If crossings in all black boxes are identically and uniformly distributed, then the boxes are statistically similar. Cut a part of each braid in the subset ω , close open tails and investigate the topological properties of resulting knots. Just such situation has been qualitatively studied in⁷, where the crumpled globule concept was formulated mainly on the basis of heuristic scaling arguments. The CG hypothesis states the following: if the whole densely packed lattice knot is trivial, then the topological state of each of its "daughter" knot is almost trivial.

It has been shown³³ that the computation of the knot complexity in the braid representation depicted in the Fig. 7 can be interpreted as the computation of the highest eigenvalue of the product of noncommutative matrices designated by black boxes.

To proceed, consider first the typical (unconditional) complexity of a knot represented by a sequence of N independent black boxes. This question is similar to the growth of the logarithm of the largest eigenvalue, λ , of the product of N independent identically distributed noncommutative random matrices.

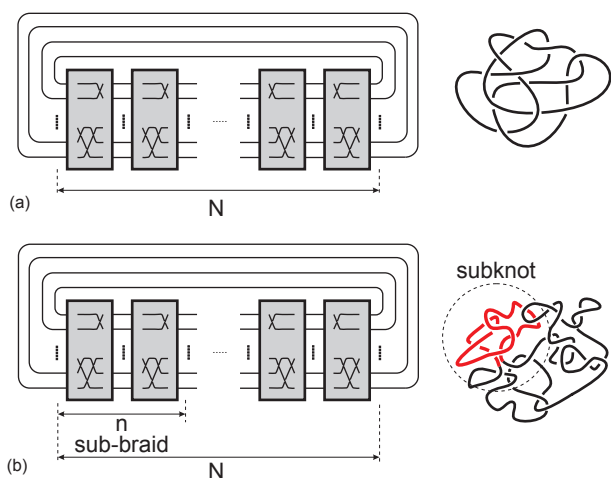


Fig. 7 Schematic representation of knots by braids: a) unconditional random distribution of black boxes produces a very complex knot; b) conditional distribution implies the whole knot to be trivial, which imposed strong constraints on complexity of any subpart of the braid.

According to the Furstenberg theorem³⁵, in the limit $N \gg 1$ one has

$$\ln \lambda(N) \sim \gamma N, \quad (1)$$

where $\gamma = \text{const}$ is the so-called Lyapunov exponent. Being rephrased for knots, this result means that the average knot complexity, \varkappa , understood as a minimal number of crossings, M , necessary to represent a given knot by the compact knot diagram, extensively grows with M , i.e. $\varkappa \sim M$. In the ordinary globule, for subchains of length $N^{2/3} < s < N$, the typical number of crossing, M , on the knot diagram grows as $M \sim s^2$, leading to the scaling behavior

$$\varkappa \sim s^2 \quad (2)$$

for the knot complexity \varkappa . This is perfectly consistent with the well known fact: the probability of spontaneous unknotting of a polymer with open ends in a globular phase is exponentially small. Following the standard scheme^{27,30}, we characterize the knot complexity, \varkappa , by the logarithm of the Alexander polynomial, $\ln[\text{Al}(t = -1.1)\text{Al}(t = -1/1.1)]$, i.e. we set $\varkappa = \ln[\text{Al}(t = -1.1)\text{Al}(t = -1/1.1)]$. As it seen from Fig. 2, the conjectured dependence $\ln \text{Al}(t = -1.1) \sim s^2$ is perfectly satisfied for ordinary (knotted) globule.

Consider now the *conditional* distribution on the products of identically distributed black boxes. We demand the product of matrices represented by black boxes to be a unit matrix. The question of interest concerns the typical behavior of $\ln \tilde{\lambda}(n, N)$, where $\tilde{\lambda}(n, N)$ is a sub-chain of first n matrices in the chain of N ones. The answer to this question is known³⁴: if $n = cN$ ($0 < c < 1$ and $N \gg 1$), then

$$\ln \tilde{\lambda}(n = cN, N) \sim \sqrt{n} = \tilde{\gamma}(c) \sqrt{N} \quad (3)$$

where $\tilde{\gamma}(c)$ absorbs all constants independent on N . Translated to the knot language, the condition for a product of N matrices to be completely reducible, means that the "parent" knot is trivial. Under this condition we are interested in the typical complexity $\tilde{\varkappa}$ of any "daughter" sub-knot represented by first $n = cN$ black boxes.

Applying the (3) to the knot diagram of the unknotted globule, we conclude that the typical conditional complexity, $\tilde{\varkappa}$ expressed in the minimal number of crossings of any finite sub-chain of a trivial parent knot, grows as

$$\tilde{\varkappa} \sim \sqrt{s^2} \sim s \quad (4)$$

with the subchain size, s . Comparing (4) and (2), we conclude that subchains of length s in the trivial knot are much less entangled/knotted than subchains of same lengths in the "unconditional" structure, i.e. when the constraint for a parent knot to be trivial is relaxed. Indeed, this result is perfectly supported by Fig. 2 which show linear grows of $\tilde{\varkappa} = \ln[\text{Al}(t = -1.1)\text{Al}(t = -1/1.1)]$ with s for the unknotted globule, while quadratic grows for the knotted globule.